Nanostructured materials for water desalination

Article *in* Nanotechnology · July 2011

DOI: 10.1088/0957-4484/22/29/292001 · Source: PubMed

11 authors, including:

Tom Humplik
Sandia National Laboratories
10 PUBLICATIONS **437** CITATIONS
SEE PROFILE

Jongho Lee
Yale University
21 PUBLICATIONS **1,201** CITATIONS
SEE PROFILE

Sean O'Hern
Exponent, Inc.
7 PUBLICATIONS **1,198** CITATIONS
SEE PROFILE

Syed Fida Hassan
King Fahd University of Petroleum and Minerals
68 PUBLICATIONS **2,398** CITATIONS
SEE PROFILE

Nanostructured materials for water desalination

2011 Nanotechnology 22 292001

(http://iopscience.iop.org/0957-4484/22/29/292001)

Nanotechnology **22** (2011) 292001 (19pp) doi:10.1088/0957-4484/22/29/292001

TOPICAL REVIEW

Nanostructured materials for water desalination

T Humplik[1], J Lee[1], S C O'Hern[1], B A Fellman[1], M A Baig[2], S F Hassan[2], M A Atieh[2], F Rahman[2], T Laoui[2], R Karnik[1] and E N Wang[1]

[1] Department of Mechanical Engineering, Massachusetts Institute of Technology, Cambridge, USA

[2] Departments of Mechanical Engineering and Chemical Engineering and Research Institute, King Fahd University of Petroleum and Minerals, Dhahran, Saudi Arabia

E-mail: tlaoui@kfupm.edu.sa, karnik@mit.edu and enwang@mit.edu

Received 5 April 2011, in final form 6 April 2011
Published 17 June 2011
Online at stacks.iop.org/Nano/22/292001

Abstract

Desalination of seawater and brackish water is becoming an increasingly important means to address the scarcity of fresh water resources in the world. Decreasing the energy requirements and infrastructure costs of existing desalination technologies remains a challenge. By enabling the manipulation of matter and control of transport at nanometer length scales, the emergence of nanotechnology offers new opportunities to advance water desalination technologies. This review focuses on nanostructured materials that are directly involved in the separation of water from salt as opposed to mitigating issues such as fouling. We discuss separation mechanisms and novel transport phenomena in materials including zeolites, carbon nanotubes, and graphene with potential applications to reverse osmosis, capacitive deionization, and multi-stage flash, among others. Such nanostructured materials can potentially enable the development of next-generation desalination systems with increased efficiency and capacity.

(Some figures in this article are in colour only in the electronic version)

1. Introduction

The increasing human population combined with exploitation of water resources for domestic purposes, industry, and irrigation has resulted in a shortage of fresh water supply in many parts of the world [1]. Only 0.5% of the 1.4 billion cubic kilometers of water in the world is accessible fresh water, which is furthermore poorly distributed across the globe [2]. There are 26 countries that do not have sufficient water resources to sustain agriculture and economic development, and approximately one billion people lack access to safe drinking water [3]. Particular regions with water scarcity include a significant portion of the Middle East, North Africa, eastern Australia, parts of Central and South Asia, and the southwestern areas of North America. In addition, the projected 40–50% growth in human population over the next 50 years, coupled with industrialization and urbanization, will result in an increasing demand on the available water resources [4]. While economic use and recycling of water for human and animal consumption can mitigate the problem to some extent [1], alternative sources of clean water are required to address this growing need.

With nearly 98% of the world's available water supply being sea or brackish water, desalination has become an important alternative source of clean water [3]. In 2009, 14 451 desalination plants were in operation worldwide with an additional 244 plants under development [5]. These plants had a total desalination capacity of almost 60 million m^3 of clean water per day; 52% of this capacity was in the Middle East, 16% was in North America, 12% in Asia, 13% in Europe, 4% in Africa, 3% in Central America, and 0.3% in Australia. In fact, the worldwide seawater desalination capacity increased by 12.4% in 2009 and is projected to grow with increasing demand for clean water.

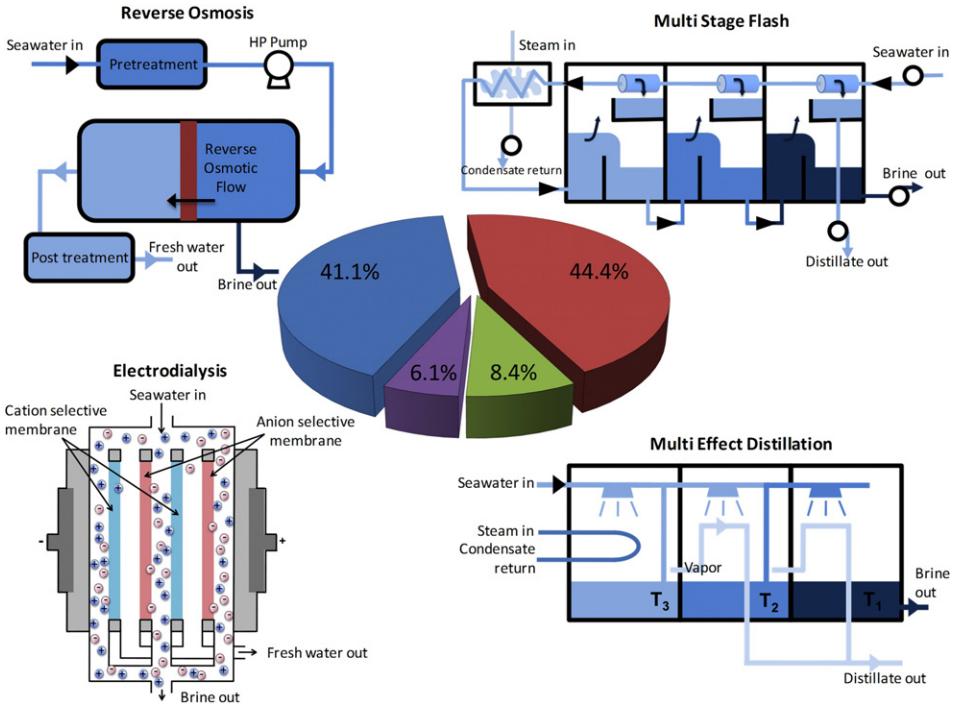

Figure 1. Schematic diagram of major desalination technologies and their relative contributions to worldwide installed capacity for seawater and brackish water desalination. MSF accounts for 44.4%, RO 41.1%, MED and other thermal methods 8.4%, ED and other methods 6.1%. Data obtained from [3, 17].

Membrane-based reverse osmosis (RO) or thermal-based multi-stage flash (MSF) and multi-effect distillation (MED) constitute over 90% of the global desalination capacity. RO plants, with typical capacities of ∼20 000 m^3 d^{-1}, account for ∼41% of the total desalination capacity while MSF plants, with typical capacities of ∼76 000 m^3 d^{-1}, account for ∼44% [3, 4]. Other technologies, such as electrodialysis, account for only a small fraction (∼5.6%) of the desalination capacity and are more suited for niche applications such as brackish and groundwater treatment [4]. The system-level schematics of the different types of desalination plants and their relative installed capacities are shown in figure 1.

The main barriers to expanding desalination technologies around the world are energy and infrastructure costs, which preclude the economical production and distribution of clean water. Energy costs range from 3.6–5.7 kWh for RO, 23.9–96 kWh for MSF, and 26.4–36.7 kWh for MED per cubic meter of clean water produced which includes pre-treatment, brine disposal, and water transport [4]. Meanwhile, these costs do not include the infrastructure and the extra maintenance costs of these large-scale processes. In 2009, desalination of 1 m^3 of seawater and brackish water cost approximately US $0.53–$1.50 and US $0.10–$1.00, respectively [6]. To meet the global demand for clean water, the total cost of desalination must decrease, which involves increasing the energy efficiency, minimizing costs associated with water pre-treatment, and decreasing the capital costs. Several technical aspects need to be addressed to realize this goal: (1) minimizing the fouling (includes biofouling due to growth of microorganisms and scaling due to precipitation of poorly soluble salts) that limits the lifetime and efficiency of desalination plants, requiring water pre-treatment, cleaning of MSF and MED plants, and cleaning or replacement of RO membranes [7]. (2) Maximizing the flux of water through RO membranes or optimizing the components of MSF and MED plants. (3) Minimizing the thermal losses in MSF and MED plants or decreasing the applied pressure in RO plants. (4) Optimizing system-level design and operation of desalination plants.

Advances in nanotechnology offer new avenues to address these challenges by increasing energy efficiency and decreasing costs associated with water desalination. While nanoscale phenomena have been identified and studied for several decades, significant progress in the ability to manipulate matter at the nanometer length scale [8] occurred in the first decade of the 21st century. These developments have opened the possibility of creating devices and systems using nanostructured materials including carbon nanotubes, nanowires, graphene, quantum dots, superlattices, and nanoshells, among other materials [9–11]. In addition to the focus on applications such as energy conversion, drug delivery, electronics, computing, structural materials, photonics, bioimaging, and biosensing [12–16], researchers have recently started investigating nanostructured materials in the context of water desalination.

The purpose of this review is to provide a perspective on state-of-the-art nanostructured materials with the potential to advance water desalination technologies. The emphasis is on materials that directly participate in the desalination process (rather than having other contributing roles such as anti-fouling), which could lead to next-generation desalination systems with increased efficiency and capacity. For detailed information on different aspects of desalination technologies,

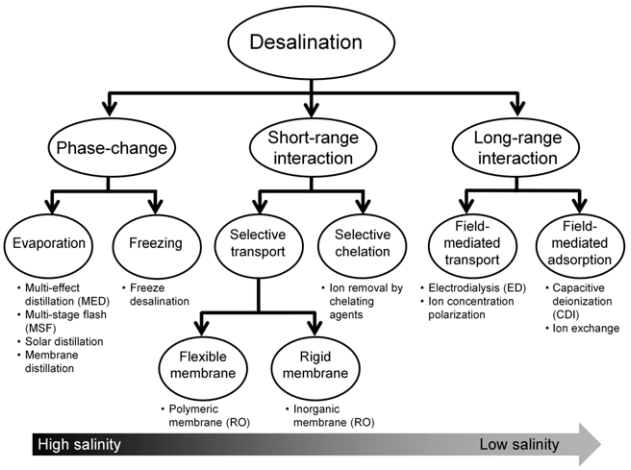

Figure 2. Overview of separation mechanisms and their use in desalination technologies. Phase-change techniques are typically more suitable for high salinity water while field-mediated techniques are better suited for low salinity water.

we refer the reader to several excellent reviews on water desalination technologies [1, 3, 4], reverse osmosis [17–20], thermal desalination processes [21, 22], fouling [23, 24], and nanomaterials for water treatment [25, 26].

This review paper is structured as follows. Section 2 gives a brief overview of the basic mechanisms that are used in water desalination. Section 3 covers the progress in membrane technology for reverse osmosis (RO) systems. This section discusses how next-generation RO membranes could utilize nanostructured materials, such as zeolites, carbon nanotubes, and graphene, and use size and charge effects to hinder the transport of salt ions while enhancing the flux of water. Section 4 focuses on approaches to desalinate water using electric fields. Specifically, this section reviews advances in electrodialysis (ED) as well as capacitive deionization (CDI). Finally, section 5 presents the potential of nanostructured surfaces for enhanced condensation and evaporation, as well as nanostructured membranes for phase-change-based processes.

2. Separation mechanisms for water desalination

Before discussing the application of nanostructured materials to different desalination technologies, it is helpful to consider some primary mechanisms for the separation of salt ions from water (figure 2). These separation mechanisms may be broadly classified into:

(1) Mechanisms involving phase change.
(2) Mechanisms involving short-range interactions with a selective material.
(3) Mechanisms involving long-range electrostatic interactions.

2.1. Mechanisms involving phase change

The separation of salt and water can occur when the feedwater to be desalinated undergoes a phase change into vapor or ice. The liquid–vapor phase transition has been widely used as a mechanism for desalination. MED utilizes brine evaporation on the surfaces of hot vapor supply pipes, while MSF involves the sequential flashing of salt water into low-pressure chambers causing the evaporation of water. Distillation techniques, e.g., solar distillation using solar thermal energy, humidification–dehumidification, or membrane distillation (where a hydrophobic membrane separates the liquid and vapor phases), all rely on evaporation [4]. In addition to the liquid–vapor phase transition, freezing has been explored for desalination since the salt preferentially remains in the liquid phase as opposed to the ice phase. Freezing desalination has many advantages including theoretically lower energy consumption due to the lower heat of fusion compared to that of vaporization, and minimal scaling problems [27]. However, the complexity of the plant design required to handle the mixture of ice and water and the contamination of product water has hindered the wide commercialization of this process [27–29].

2.2. Mechanisms involving short-range ($< \sim 1$ nm) interactions with a selective material

Short-range interactions between water molecules or ions with another material involving a combination of steric, dispersion, dipole and electrostatic interactions can also be used for desalination. These interactions can enable desalination by the preferential transport of either water molecules or ions through a selective material, or by chelation or adsorption/absorption of ions to a chelating material. While methods that use chelation or adsorption are more suitable for the removal of trace metals (e.g., removal of boron [30, 31]), transport through selective media is widely used for desalination in RO. The selective materials may be further classified into flexible polymeric materials that rely on selective sorption and transport, and rigid materials that use a molecular sieving effect based on steric exclusion. The process of sorption comprises adsorption (mobile molecules affix themselves to the material interface) followed by absorption (molecules enter the material). Polymeric RO membranes exhibit selective sorption as water preferentially enters the material; a second level of selectivity arises due to the higher diffusivity of water molecules compared to ions. While flexible polymeric membranes cannot completely rely on size exclusion, rigid membranes with sub-nanometer pores can potentially act as molecular sieves for separation of the smaller water molecules ($\sim$3.3 Å van der Waals diameter) from the larger hydrated salt ions ($\sim$7–8 Å).

2.3. Mechanisms involving long-range ($> \sim 1$ nm) electrostatic interactions

The presence of electrical charges on ions and the absence of a net charge on water molecules enable the use of long-range electrostatic fields to selectively exert forces on ions. Electric fields are capable of depleting, accumulating, or transporting ions; the discipline concerned with these phenomena is known as electrokinetics [32]. Thus, charged surfaces attract ions of the opposite charge while repelling ions of like charge, forming an electric double layer (EDL). The thickness of the EDL

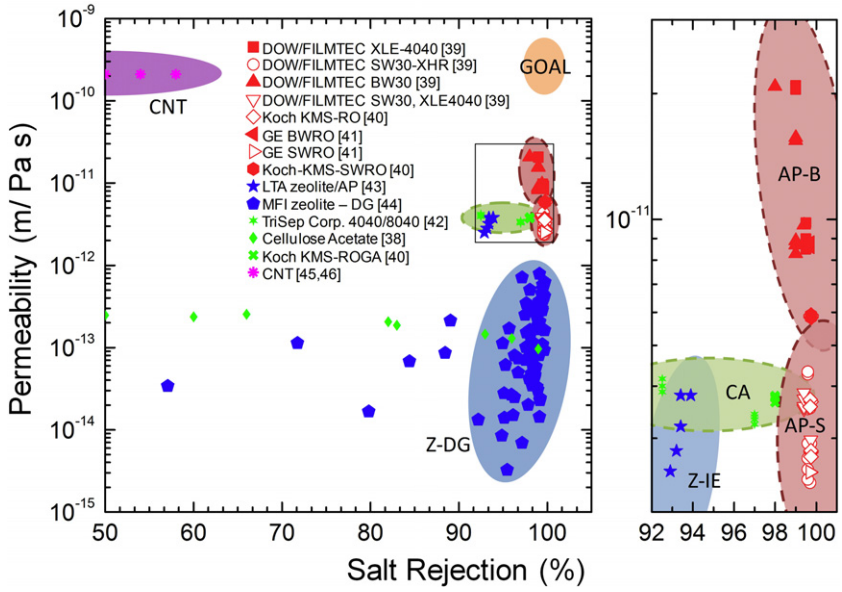

Figure 3. Comparison of permeability and salt rejection of commercial RO membranes and nanostructured membranes reported in literature. Open symbols represent seawater/high salinity conditions while closed symbols represent brackish/low salinity conditions. Regions enclosed by dashed lines represent commercially available membranes. AP-B: aromatic polyamide (brackish); AP-S: aromatic polyamide (seawater); CA: cellulose acetate (brackish); CNT: carbon nanotube (brackish); Z–DG: zeolite, direct growth method (brackish); Z–IE: zeolite, interfacially embedded (brackish). The ideal RO membrane characteristics are indicated by the orange region (goal). A magnified view of the outlined box is shown to the right. Data obtained from [38–46]. 1 m (Pa^{-1} s^{-1}) = 3.6×10^{11} l/(m^2 h bar).

depends on the salt concentration, which typically ranges from ~1 μm for deionized water to less than 1 nm for seawater. Therefore, ions can be preferentially adsorbed on charged surfaces or selectively transported through membrane pores as a result of these longer-range electrostatic interactions that are used in CDI and ED for desalination.

3. Reverse osmosis (RO)

RO is a growing seawater desalination technology due to the lower energy costs when compared to MSF systems. Recent developments in membrane technology, including biofouling reduction, scaling inhibitors, and materials synthesis, along with energy recovery devices, have decreased the energy consumption of RO plants to 3.6–5.7 kWh m^{-3}, as compared to 23.9–96 kWh m^{-3} for MSF plants [17]. Currently, RO plants account for ~41% of the world's desalination capacity and ~80% of the number of operating plants [3, 6]. RO plants are now the most commonly installed desalination systems in the world accounting for ~75% of newly built capacity, except for areas with vast energy reserves or high salinity feedwater.

In RO, desalination is achieved by applying high pressure to feedwater, forcing it through a semi-permeable membrane that permits the flow of water molecules, while restricting the flow of salt ions. For desalination to occur, the applied pressure must exceed the osmotic pressure of the feedwater [6, 17, 33, 34]. To achieve reasonable water fluxes of 12–17 l(m^{-2} h^{-1}) for seawater (>35 000 ppm total dissolved solids or TDS) and 12–45 l(m^{-2} h^{-1}) for brackish water (1000–5000 ppm TDS), the pressures are 55–65 bar and 10–30 bar, respectively [6].

State-of-the-art RO systems utilize asymmetric polymeric membranes comprising a semi-permeable active layer supported by a porous layer. Under applied pressure, water transports through these membranes via sorption of the water molecules into the active layer followed by coupled diffusion and convection [6, 33–36]. Therefore, to achieve high water flux, a high permeability of the membrane is desired while maintaining high salt rejection. Membrane permeability depends on the membrane material, but the flux of water is also impacted adversely by biofouling and scaling. Furthermore, concentration polarization, i.e., accumulation of salt near the membrane, which also decreases the water flux, should be minimized by appropriate system design [37]. An ideal RO membrane thus maximizes flux, has high salt rejection, and resists scaling, biofouling, and degradation by chemicals (e.g., chlorine) that reduce biofouling [6].

RO membranes were initially developed using cellulose acetate and commercialized in the 1960s, but offered relatively low fluxes and were subject to biological degradation [38]. Current state-of-the-art RO membranes are asymmetric polyamide and thin-film composite membranes fabricated using interfacial polymerization. These membranes consist of a hierarchical structure where a thin (100–1000 nm) polyamide selective layer is fabricated on a porous polysulfone layer that offers mechanical support and minimizes pressure drop [17]. The permeabilities and salt rejection of some commercial desalination membranes under laboratory test conditions are shown in figure 3.

While RO systems have already been commercialized, improving water flux, salt rejection, and resistance to fouling and degradation of the membranes are required to advance this technology to meet future needs. Higher permeability

membranes may enable operation closer to the ideal osmotic pressure, thereby decreasing the energy cost for a given membrane area and capacity; alternatively, such membranes may reduce capital cost or plant size by requiring less membrane area for a given desalination capacity. However, the coupling between flux, salt rejection, and other properties such as mechanical stability and fouling resistance requires careful optimization of the membrane material, which is particularly challenging as improving one factor tends to adversely affect the others [17]. Researchers have extensively explored various combinations of polymeric materials, as well as different synthesis procedures and modification techniques to optimize membrane performance [18, 19]. Some of the issues have been addressed by providing macroscopic solutions, e.g., feedwater pre-treatment to minimize membrane fouling. These aspects are covered extensively in recent reviews on RO [17, 18]. While significant advances have been made in polymeric RO membrane technology, new approaches beyond the optimization of polymeric materials could be exploited to develop next-generation membranes.

Advances in nanotechnology have enabled unprecedented control over the fabrication of nanostructured materials, and in particular, the ability to create well-defined, size-selective, nanostructured filtration membranes. In contrast to polymeric membranes with flexible chains that do not form well-defined pores, a rigid, size-selective membrane with pore sizes in the sub-nanometer regime is expected to allow water molecules to pass through, while impeding the passage of ions that have a larger effective diameter due to their hydration shells [47, 48]. For example, the diameter of a hydrated sodium ion is ∼7.6 Å; theoretically, if the pore diameter is smaller than that of a solvated ion but larger than a water molecule, the pore could act as a molecular sieve. Since a significant energy barrier must be overcome to strip the ion of its solvation shell (∼1709 kJ mol^{-1} for Na^+) [49, 50], applying a pressure greater than the osmotic pressure on the feedwater will force the water molecules through such pores while impeding the passage of ions. In addition to selectivity through steric exclusion, electrostatic and van der Waals interactions may also play an important role or may be harnessed to achieve the desired selectivity.

Nanostructured materials that are promising for desalination include zeolites [51, 52], carbon nanotubes [45, 46], and graphene [53–55], which can be synthesized to have non-tortuous pores on the order of 1 nm or less and can be fabricated into macroscopic arrays. Figure 3 summarizes the current performance of nanostructured materials that are in research or are commercially available, compared to polymeric RO membranes. In the following sections, we discuss in detail the progress in the fabrication and understanding of the transport characteristics of these materials to achieve improved RO membranes for the development of efficient desalination.

3.1. Zeolites

Zeolites are aluminosilicate minerals with a microstructure composed of 3–8 Å pores (figure 4). Zeolite crystals occur naturally or can be synthesized in a laboratory environment using a high temperature furnace and an autoclave [56].

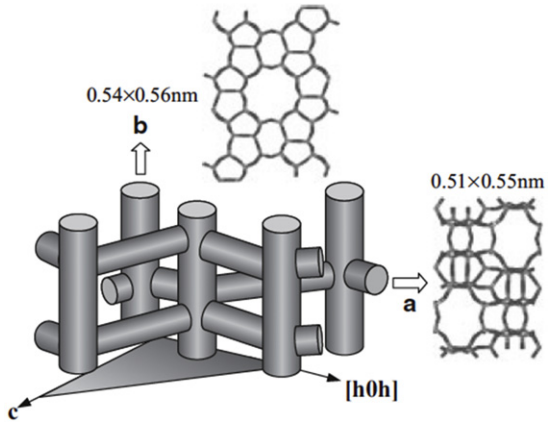

Figure 4. Schematic diagram of the MFI zeolite morphology. Adapted with permission from [58] (Copyright 2004, John Wiley and Sons).

Crystal sizes can be controlled from a few nanometers to centimeters by varying synthesis temperature and time [56]. Properties such as adsorption characteristics, geometry, ion exchange capabilities, and catalytic behavior differ amongst the zeolite crystal families and can be tailored to a specific application by using the correct composition [56]. Porosity varies among zeolites, typically ranging between 30–40%. The combination of high porosity and high active surface area has led to significant zeolite research for catalytic applications. In commercial applications, the most common use for zeolites is as adsorbents during various chemical processes [57].

Since most zeolites have a tight pore distribution less than the diameter of a hydrated salt ion, a membrane created from these crystals has the potential to completely reject salt ions while permitting water molecules to permeate through. Molecular dynamics (MD) simulations have provided mechanistic insights into these processes. Murad and Lin investigated water–ion separation using a single ZK-4 zeolite with 4.4 Å pore diameters in a NaCl/water solution [59, 60]. The solvated ions were too large to pass through the pores and only water molecules could flow through the zeolite.

These MD simulations have since motivated researchers to fabricate zeolite-based membranes for RO and experimentally investigate the possibility of achieving high flux with excellent ion rejection. Li *et al* [51] used hydrothermal synthesis to develop 0.5–3 μm thick membranes consisting of hydrophobic MFI (mordenite framework inverted) type zeolites with an average pore diameter of 5.6 Å on a porous α-alumina support (figure 5(a)). Under an applied pressure of 2.07 MPa (20.7 bar) and with 0.1 M NaCl feedwater, the membranes rejected 76% of Na^+ ions while permitting a water flux of 0.112 kg (m^{-2} h^{-1})(∼0.11 l (m^{-2} h^{-1})). This lower rejection was attributed to ions transporting across nanometer-sized interstitial defects created during the membrane synthesis process. In later work, Li *et al* decreased the silicon/aluminum ratio of the zeolite, which decreased the hydrophobicity and increased the flux to 10.21 (m^{-2} h^{-1}) with an applied pressure of 3.5 MPa (35 bar) and 0.1 M NaCl feedwater [44]. Ion rejection also improved dramatically from ∼76% to 98.6% (figure 5). However, as the salt concentration of the solution

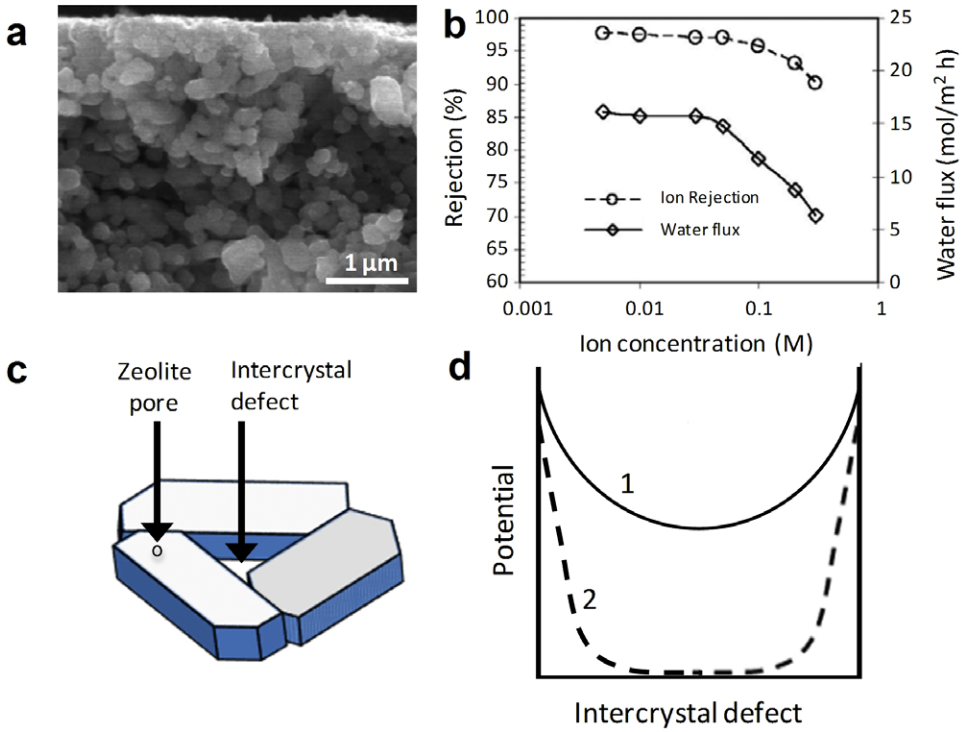

Figure 5. (a) Cross-sectional view of a zeolite membrane grown directly on porous α-alumina support. Adapted from [44] (Copyright 2009, Taylor and Francis). (b) Experimental results of ion rejection and water flux for direct growth zeolite membranes as a function of ion concentration. Adapted from [61] (Copyright 2008, Elsevier). (c) Schematic of intercrystalline pore structure of direct growth zeolite membranes. Adapted from [51]. (d) Schematic of overlapping of the EDL between zeolite crystals at low salt concentration (solid line) and high salt concentration (dashed line). Adapted from [51].

increased, the salt rejection decreased considerably to ~90% for a 0.3 M NaCl solution [52]. These results suggest that the salt rejection depended on the formation and size of EDLs at the surface of the intercrystalline defects: in low salt concentrations, the EDLs can overlap and prohibit the transport of salt ions, while, in high salt concentrations, EDLs become thinner and no longer overlap, allowing ions to pass through the intercrystalline defects (figure 5). These experimental results showed that nanometer-sized intercrystalline defects controlled the majority of ion transport and presented a challenge for the fabrication of zeolite membranes.

In addition to synthesizing zeolites directly onto a ceramic support, zeolites have also been incorporated into polymeric RO membranes. Jeong *et al* synthesized thin polymer-composite (TFN) membranes interfacially embedded with ~100 nm cubic LTA (Linde Type A) zeolite crystals with 4.4 Å diameter pores [43], shown in figure 6. These hydrophilic zeolites were chosen to create preferential flow paths for water to permeate through while also simultaneously rejecting the transport of ions.

The membranes were characterized for permeability and salt rejection with increasing zeolite content using a 2000 ppm $NaCl/MgSO_4$ (~0.03 M) solution and an applied pressure on the feed side of 1.24 MPa (12.4 bar). Increased water fluxes were demonstrated with increasing zeolite weight percentage. Additionally, membranes with embedded zeolite always showed higher permeability when compared to experimental thin-film composite (TFC) membranes without zeolites while maintaining high salt rejection (figure 6). However, even with the optimal zeolite loading of ~40%, the water flux was found to be lower than some commercial state-of-the-art RO membranes. Although further work is needed to optimize the zeolite-loaded membrane structure and synthesis techniques, the permeability and salt rejection results indicate the potential of zeolite-based membranes for RO.

However, a challenge with the zeolite membranes described above is that water molecules and ions can permeate around the zeolite crystals. In this configuration, it is difficult to determine the role that zeolites have in water transport and salt rejection. Additionally, if salt can transport around the zeolite crystal, perfect salt rejection cannot be achieved. Further research is needed to determine the specific transport mechanisms within the sub-nanometer zeolite pores and in fabricating membranes that limit the transport to the intrinsic zeolite pores. These types of studies will help clarify the benefit of zeolites for RO desalination.

3.2. Carbon nanotubes (CNTs)

CNTs are an allotrope of carbon consisting of rolled-up sheets of graphitic layers [62]. CNTs are attractive for applications ranging from structural materials to electronics and energy storage due to their excellent thermal and electrical conductance, mechanical strength, and unique electronic

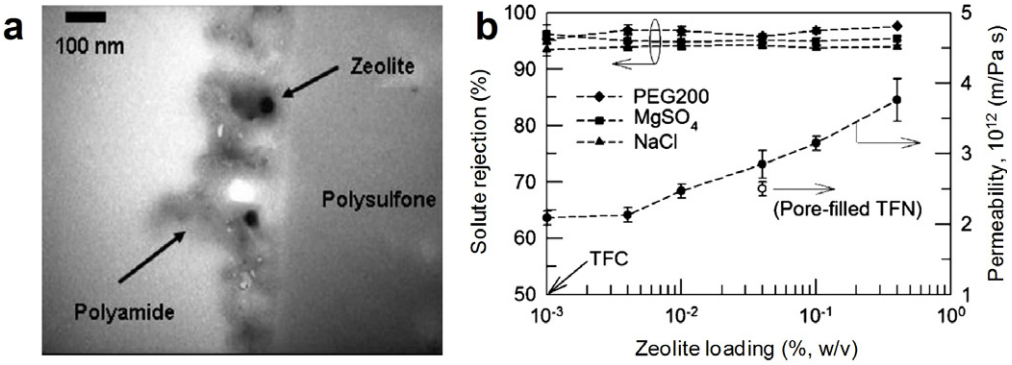

Figure 6. (a) TEM micrograph of hand-cast nanocomposite membrane incorporating LTA zeolites in polyamide with a polysulfone support layer. (b) Experimentally measured solute rejection and permeability of the zeolite/polyamide composite membranes. The membranes exhibit increasing permeability with increasing zeolite loading while the solute rejection remained approximately constant. Open symbol indicates a zeolite pore-filled (non-calcined) TFN membrane. The TFC arrow corresponds with 0% W V^{-1} zeolite loading. Other arrows indicate data corresponding to the axes. Both parts adapted with permission from [43] (Copyright 2007, Elsevier).

properties [63–72]. Advances in synthesis procedures have recently enabled tight control of the diameter of CNTs down to 1.6 nm and lengths up to a few centimeters [73–77]. Such controlled synthesis techniques have led to the recent discovery of high water fluxes through CNT membranes [46, 78], opening the possibility of using such CNT membranes for RO [45].

Both MD modeling [79, 81] and experiments [46, 78] have demonstrated that water fluxes through CNTs can be several magnitudes greater than those predicted by continuum hydrodynamics. MD simulations performed by several groups have provided mechanistic insights into the ultrafast water transport. Kolesnikov *et al* first showed that confinement of water molecules in a CNT leads to an 'ice shell plus water chain structure,' which suggests that the interactions between the water molecules are stronger than the interactions of the water molecules with the CNT wall [82]. Joseph and Aluru subsequently examined the transport of water molecules through CNTs with varying degrees of hydrophobicity and surface roughness [79]. The results (figure 7) showed that both hydrophobicity and the atomistic smoothness of CNT walls are necessary for fast water transport, resulting in nearly frictionless flow. More recently, Falk *et al* discovered that the friction coefficient between the water molecules and the CNT wall is highly dependent upon the curvature of the graphitic surface of the CNTs [80]. Using MD simulations, they demonstrated that the curvature modulates the interaction energy landscape of water molecules with the CNT such that the friction decreases with decreasing CNT diameters, and vanishes below a CNT diameter of 0.5 nm. Interestingly, the simulations indicated that the friction was higher for water molecules interacting with the outer surface of the CNTs.

Fast mass transport in CNTs was experimentally verified by Majumder *et al* [78] and Holt *et al* [46], who fabricated CNT membranes by filling the interstitial space of an array of vertically aligned CNTs with polystyrene and silicon nitride, respectively (using procedures described in [83, 84], respectively). Majumder *et al* measured the flow rate of water, ethanol, isopropanol, hexane, and decane through 7 nm multi-walled CNTs under 1 bar of pressure. The liquid flux through the membrane was 4–5 orders of magnitude greater than the flux predicted by continuum hydrodynamics and interestingly, did not decrease with increasing fluid viscosity. Holt *et al* measured the pressure-driven flow of water through 1.6 nm double-walled CNTs with similar results.

While the studies reported high flux through the CNT membranes, the CNT diameters were too large to act as molecular sieves for excluding salt ions. Therefore, membranes comprising CNTs with chemically modified tips with charged groups were developed to achieve a high salt rejection capability through electrostatic repulsion (figure 8). Fornasiero *et al* functionalized the pore entrance of these CNT arrays with carboxyl groups, which successfully achieved 40–60% salt rejection for dilute (<0.01 M) salt concentrations of KCl, and nearly 100% salt rejection for dilute solutions of $K_3Fe(CN)_6$ [45]. The higher rejection ratio for $K_3Fe(CN)_6$ may be attributed to the greater electrostatic repulsion between the trivalent anion and the carboxyl groups at the CNT entrance. The salt rejection was poor for higher salt concentrations that correspond to a smaller electrostatic Debye screening length; above 10 mM concentration of KCl, the salt rejection was almost zero.

3.3. Graphene

Graphene is another carbon-based material that has recently received attention as a potentially selective material for membranes. Graphene is a single layer of graphite with atomistic thickness, consisting of a lattice of hexagonally arranged sp^2-bonded atoms [85, 86], which has attracted attention for electronic applications due to its unique properties [85]. In addition to its electronic properties, graphene exhibits a high breaking strength [87] and impermeability to molecules as small as helium in its pristine state [88]. These properties suggest the potential of graphene to create ultrathin high flux membranes with size-tunable pores that can act as molecular sieves. Furthermore, single or few-layer graphene sheets on large areas have been synthesized and 30 inch sheets have been transferred on a roll-to-roll basis [89], indicating the feasibility of large-scale membrane fabrication.

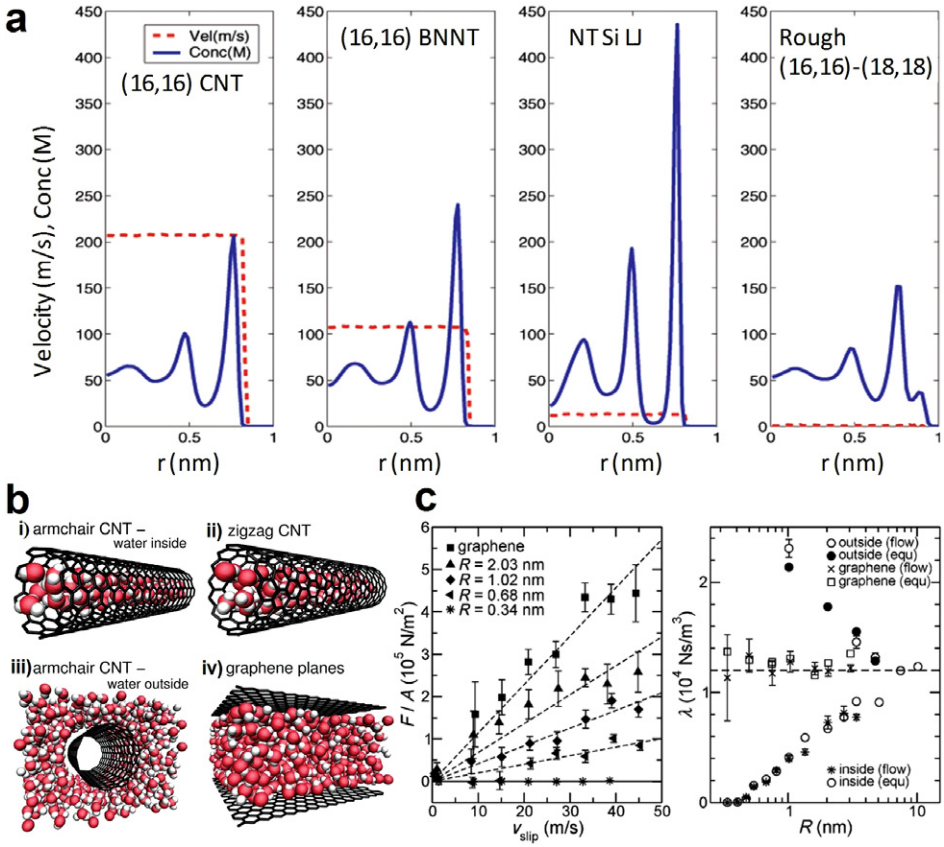

Figure 7. (a) Velocity and concentration of water molecules as a function of radial distance from the center of four types of nanotubes (left to right): (16, 16) CNT, (16, 16) boron nitride nanotube (BNNT), hydrophilic nanotube with silicon Lennard-Jones parameters (NT Si LJ), and rough CNT comprising alternating (16, 16) and (18, 18) segments. Adapted with permission from [79] (Copyright 2008, American Chemical Society). (b) Flow of water (i) inside armchair CNT, (ii) inside zigzag CNT, (iii) outside armchair CNT, and (iv) between graphene sheets. Adapted with permission from [80] (Copyright 2010, American Chemical Society). (c) Shear stress due to friction (F/A) of water as a function of slip velocity at the CNT surface for various diameters of CNTs (left). Square symbols show graphene slab with a wall-to-wall distance of 2.33 nm. Evolution of the friction coefficient λ with the confinement R for water inside/outside CNT (with a diameter $d = 2R$) and between graphene sheets (at a distance $H = 2R$) (right). Adapted with permission from [80] (Copyright 2010, American Chemical Society).

Several groups have studied the effects of induced defects on the electrical properties of graphene [93]. Recent simulations and experimental studies suggest that sub-nanometer pores can be controllably generated by methods such as oxidation [94], electron beam irradiation [95, 96], ion bombardment [97–101], or by doping [102]. Earlier studies that focused on graphene as an electronic material led to more recent studies that explored the transport of gases or ions through pores in graphene membranes [53, 55, 92]. Sint *et al* [55] studied the transport of ions through ∼0.5 nm pores in graphene terminated with nitrogen or hydrogen using MD simulations. They observed that the N-terminated pore allowed the passage of Li^+, Na^+, and K^+ ions, while the H-terminated pore admitted Cl^- and Br^-, but not F^-. Interestingly, contrary to allowing smaller ions to pass more easily, they observed that the smaller ions had the lowest passage rates due to their strongly bound hydration shells. Furthermore, the study showed that the polar/charged terminal groups of the pore assisted in the removal of water molecules from the hydration layer, similar to the case of protein ion channels. More recently, Suk and Aluru explored the rate at which water molecules transport across 0.75–2.75 nm diameter pores in graphene membranes, and compared it with 2-10 nm long carbon nanotubes (CNTs) with similar diameters [92]. The flux through graphene pores was found to be within a factor of two of that through CNTs, with a significant resistance to transport arising from the entrance regions of the pore (figure 9). These studies indicate the potential of graphene membranes for water desalination with fluxes up to an order of magnitude higher than polymeric RO membranes. However, while graphene pores have been used for DNA detection and ionic currents across these membranes have been reported [103–105], experimental measurements of water transport and salt rejection remain to be realized.

3.4. Summary

Nanostructured materials including zeolites, CNTs, and graphene offer the possibility of high flux molecular sieving membranes for water desalination. The ability to control the pore size in the sub-nanometer regime is critical for the proper functioning of such membranes. At these length

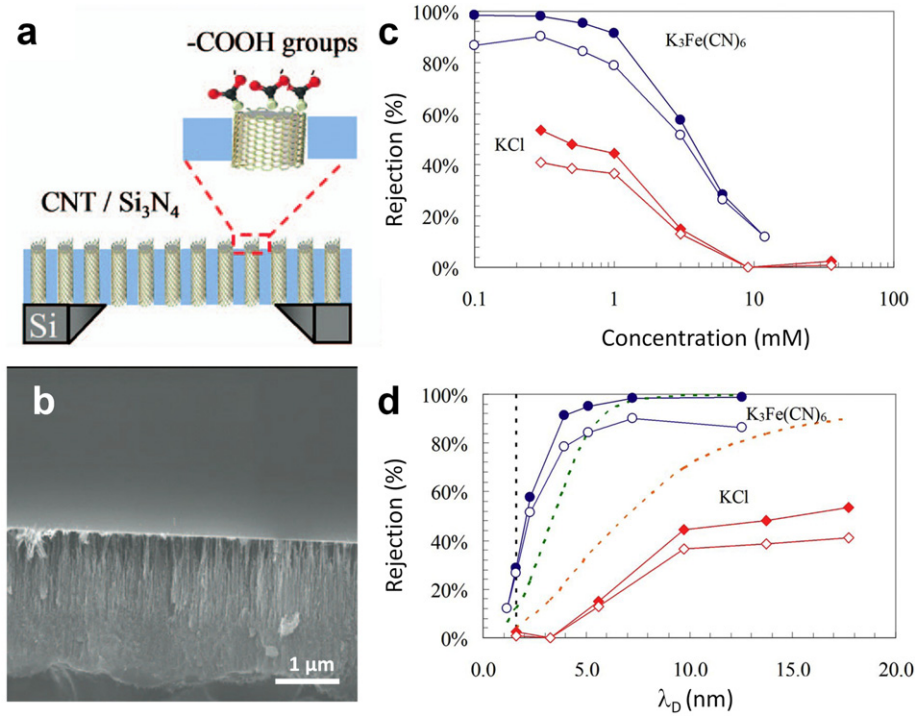

Figure 8. (a) Schematic of CNT membrane with functionalized 1.6 nm openings. (b) SEM micrograph of the membrane cross-section. Salt rejection as a function of feedwater salt concentration (c) and Debye length (d). Adapted with permission from [45] (Copyright 2008, National Academy of Sciences (USA)).

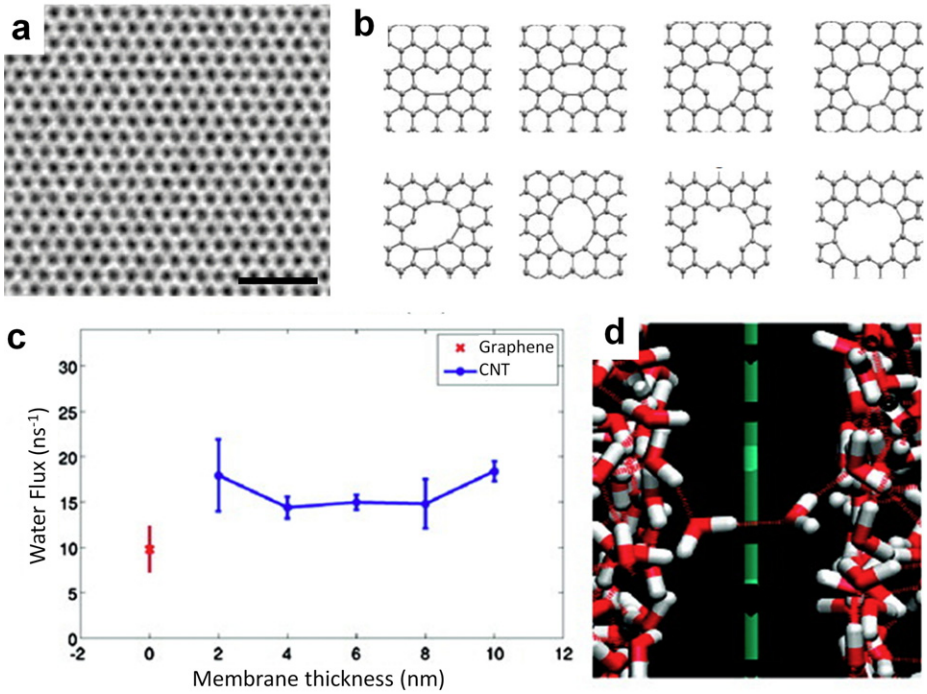

Figure 9. (a) HRTEM image of graphene lattice. Scale bar is 1 nm. Adapted with permission from [90] (Copyright 2008, American Chemical Society). (b) Simulated atomic structures of defective graphene, 1–8 atomic vacancies, respectively. Adapted with permission from [91] (Copyright 2007, Japan Society of Applied Physics). (c) MD simulations of water flux through 0.75 nm pore in graphene under 100 MPa applied pressure; permeability is of the same order of magnitude as CNTs. Adapted with permission from [92] (Copyright 2010, American Chemical Society). (d) Visualization of single-file water molecule translocation through the same pore as in (c). Adapted with permission from [92] (Copyright 2010, American Chemical Society).

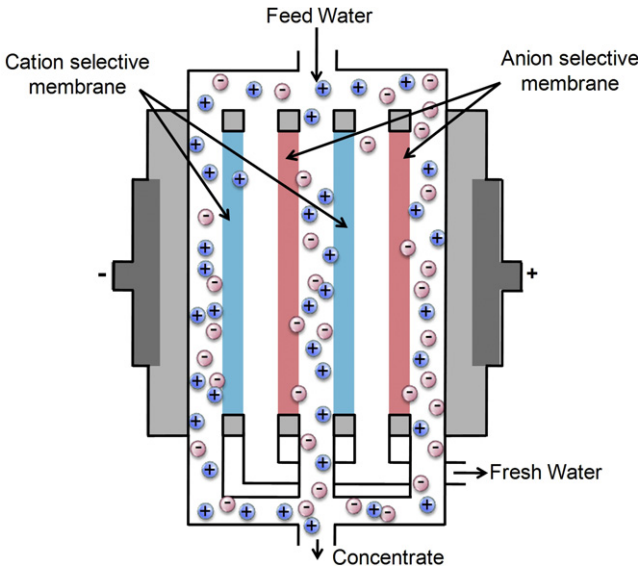

Figure 10. Schematic of ED desalination system with cation (blue) and anion (red) selective membranes.

scales, unique transport properties arising due to steric and electrostatic interactions and ultrafast transport can be utilized. The integration of these materials into large area membranes and measurement of their transport characteristics remain challenging. Aside from these materials, other nanostructures have potential uses for desalination. For example, Zhou *et al* synthesized a porous polymer membrane using lyotropic liquid crystals with an interconnected pore structure and a nominal pore size of ∼0.75 nm [106]. Biological protein channels such as aquaporins also exhibit high flux and selective ionic or water transport [107–111]. While significant research is needed, the novel transport phenomena in nanostructured materials provide ample opportunities to improve RO membranes.

4. Charge-based desalination techniques

The presence of charged species in water promises the use of various electric-field-driven separation technologies for desalination. While the most prominent of these technologies today is electrodialysis (ED), other techniques such as capacitive deionization (CDI) that exploit the same governing physics—electromigration of ions under an applied electric field—have received recent interest to achieve salt separation. These charge-based separation systems have advantages over other existing desalination techniques in the case of low salinity water, requiring lower pressures and energies compared to RO and MSF, respectively [112]. These systems are suitable for the small-scale production of drinking water and ultra-pure water [112–114].

4.1. Electrodialysis (ED)

ED was first developed for water desalination approximately half a century ago and was commercially introduced in 1953, which is about 10 years before RO. In ED, feedwater streams are separated by a series of negatively charged cation and positively charged anion selective membranes in an alternating pattern (figure 10).

When an electric field is applied across the membranes, cations and anions migrate in opposite directions through their respective membranes into the concentrate channels (figure 10). This process reduces the concentration of salt in the feed streams while increasing its concentration in the waste streams. The required electrical power depends on the salt concentration in the feedwater, and therefore ED is less efficient than RO at salt concentrations over ∼5000 ppm TDS [4]. The development of electrodialysis reversal (EDR) (electric field is periodically reversed) and spacers (for mixing enhancement) has mitigated membrane scale formation and concentration polarization and resulted in increased water recovery. Previous research has also focused on achieving high permselectivity of the ion selective membranes, low electrical resistance, low fabrication cost, and mechanical and chemical stability of membranes [115] to improve membrane performance. However, due to dramatic improvements in RO membranes, ED has become more of a niche technology, now accounting only for 5.6% of the world's desalination capacity [3].

4.2. Capacitive deionization (CDI)

With the availability of high surface area electrodes for energy storage, water desalination using CDI has emerged as an active research topic [114]. In CDI, salt water passes across high surface area electrodes. During this process, voltage applied to the electrodes causes ions to electromigrate and adsorb on the electrode surfaces to shield the surface charge, thereby reducing the concentration of salt in the solution. The desalinated water is removed from the system and new feedwater is introduced. The electrodes are then discharged such that the ions desorb from the electrodes resulting in brine, which is removed and replaced with fresh feedwater, thus continuing the cycle (figure 11). Several stages may be employed to achieve adequate depletion of salt [112, 114]. When the ions electrostatically adsorb on the electrodes, part of the energy expended during application of the electric potential is stored due to capacitance of the EDL. By releasing the ions from the EDL into a purge (waste) stream, part of this energy can be reclaimed while the electrode surfaces are cleaned for future adsorption cycles. The process has the potential to be highly efficient, especially for low salt concentration feedwater such as brackish water, because this technique essentially charges and discharges a series of electrochemical capacitors. For high salinity feedwater, the capacitance of the electrodes becomes a limiting factor and the use of CDI for desalination becomes uneconomical [112].

The main challenges for the development of economical CDI systems are high energy consumption related to parasitic reactions at the electrodes, inadequate electrical connectivity to the high surface area electrodes, and limitations on electrode materials and geometries that lead to trade-offs between maximizing the surface area and minimizing the distance for ionic electromigration. Although macroscopically CDI appears to be simple, the ion transport locally within the

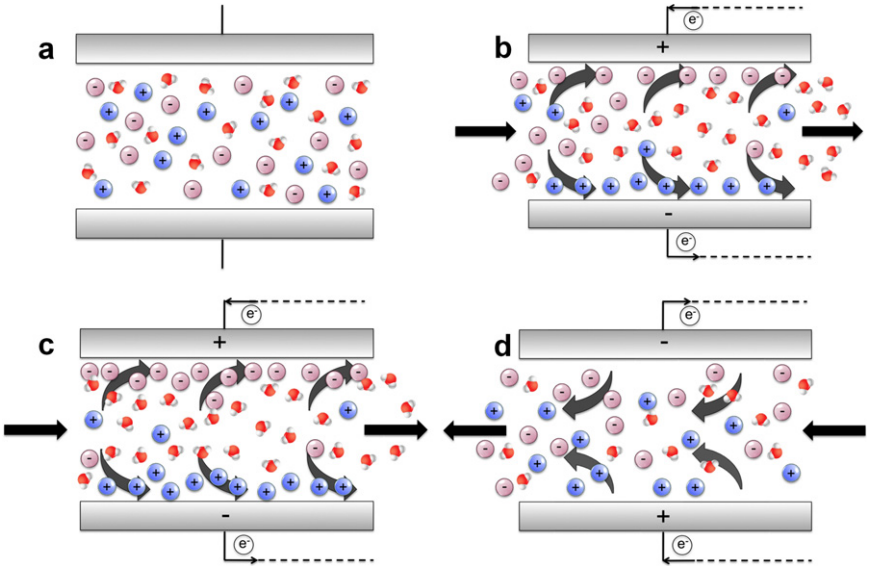

Figure 11. Schematic of CDI process. (a) Feedwater in CDI cell before voltage is applied. (b) Voltage is applied and ions begin to migrate according to the applied potential. (c) Electrodes become saturated with ions and desalinated stream is purged from the CDI cell. (d) After fresh feedwater enters the cell, the applied voltage is partially reversed so that ions desorb from the electrodes resulting in brine that is discharged, and the next cycle begins.

electrodes is not well-understood. The modeling efforts for CDI are challenging because classical electrokinetic theory cannot be used due to the large applied surface potentials of approximately 1 V (compared to the thermal voltage of 25.7 mV at 25 °C), long charging times, complicated electrode geometries, and small, confined pores. Recently, studies have revisited and modified standard Poisson–Boltzmann theory for the EDL [32] to account for steric effects of the ions at large voltages to better understand the charge build-up in the EDL [3, 120–123]. Additionally, models have started to address the dynamics of electrode charging, by coupling electrokinetic theory with ion diffusion [124, 125]. These advancements offer insights into identifying optimal electrode geometries and operating conditions in future CDI systems.

Despite these recent modeling developments, the synthesis of electrode materials that provide a high surface area, good electrical conductivity, and control of Faradaic reactions remains a challenge. Significant research efforts in CDI have focused on novel electrode synthesis and the characterization of electrode materials with an emphasis on hierarchical microstructured and nanostructured electrodes to achieve the high surface areas required for the electrosorption of a significant number of ions. Figure 12 shows SEM micrographs of carbon-based nanostructures currently under investigation for CDI including (a) carbon nanotubes/nanofibers (CNT/CNF), (b) carbon cloth films, (c) carbon aerogel matrices, and (d) mesoporous carbon matrices.

4.2.1. Carbon aerogels. Although CDI was first investigated in the 1960s and 1970s [126], CDI research reemerged in the 1990s with Farmer *et al* investigating carbon aerogel electrodes with surface areas ranging from 400–1100 $m^2\ g^{-1}$ [127–129]. Carbon aerogels are highly cross-linked, solid networks of covalently bonded carbon particles derived from a sol–gel synthesis process. The aerogels can have porosities greater than 50% while maintaining pore sizes on the order of 100 nm or less [129]. Carbon aerogels have been used to successfully remove 95% of a 100 $\mu S\ cm^{-1}$ NaCl solution (approximately 1 mM) before saturating the electrodes [130]. One limitation of carbon aerogels is that although they have a large surface area, much of this large surface area is due to micropores (less than 2 nm) that are inaccessible to ions [116]. While researchers continue to investigate carbon aerogels [131–136], the focus has shifted to other carbon-based materials with larger pore sizes (∼2–50 nm) that are accessible to solvated ions. Many of these studies investigate modifications of such carbon-based materials to obtain better pore size distributions to enhance ion capture in CDI. These materials include activated carbon, activated carbon cloth, CNTs, and more recently ordered mesoporous carbons, which promise high electrical conductivity and high surface area.

4.2.2. Activated carbon. Activated carbon, a highly porous form of carbon derived by the activation of pyrolysis products of carbonaceous materials such as coconut shell and wood, has a high specific surface area of ∼500–2300 $m^2\ g^{-1}$ [137]. Activated carbon has therefore found use in supercapacitors as well as CDI [138–141]. With activated carbon-based electrodes, one major challenge for water desalination is the hydrophobicity of the electrode material since a hydrophobic polytetrafluoroethylene (PTFE) binder is required to maintain the material consistency. Supercapacitors typically use non-aqueous electrolytes so that the capacitors can charge to voltages larger than the 1.23 V required for the electrolysis of water, and electrode wetting is consequently not a major concern. However, electrode wetting is especially critical for CDI. Thus, some efforts have focused on enhancing the wettability of activated carbon. Lee *et al* added ion

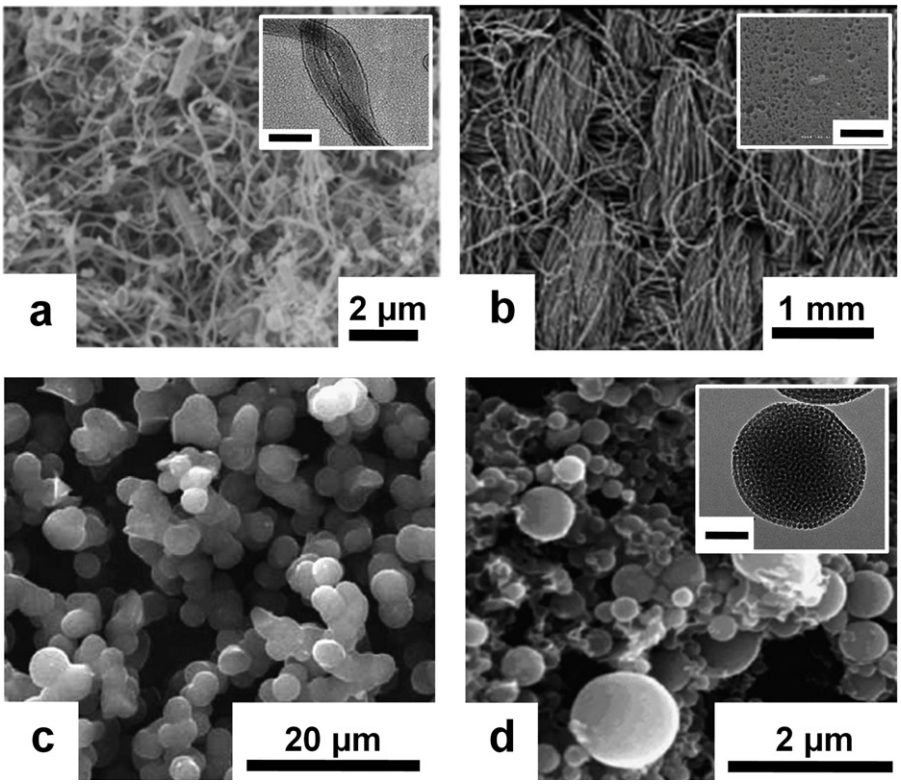

Figure 12. Micrographs of high surface area electrode materials for CDI. (a) SEM micrograph of carbon nanotube/nanofiber composite film. Inset: TEM image of CNT/CNF composite. Scale bar is 100 nm. Adapted with permission from [116] (Copyright 2006, American Institute of Physics). (b) SEM micrograph of activated carbon cloth film. Inset: high resolution SEM micrograph of activated carbon cloth microstructure. Scale bar is 250 nm. Adapted with permission from [117] (Copyright 2006, Elsevier). (c) SEM micrograph of carbon aerogel matrix. Adapted with permission from [118] (Copyright 2006, Elsevier). (d) SEM micrograph of ordered mesoporous carbon matrix. Inset: TEM micrograph highlighting ordered mesoporous structure. Scale bar is 100 nm. Adapted with permission from [119] (Copyright 2005, Elsevier).

exchange resin to standard activated carbon and PTFE slurries to increase the electrode hydrophilicity, decreasing the contact angle of the electrode from 115° to 75° and 85° with 24% and 36% ion exchange resin, respectively. Water was easily wicked into these electrodes, yielding a 35% improvement in the desalinated water production over the standard activated carbon electrodes [141].

4.2.3. Activated carbon cloth. Activated carbon cloths (ACCs) have also received significant attention due to their large surface areas. Unlike activated carbon electrodes, they do not contain any PTFE binder. Activated carbon cloths are typically chemically activated cloth comprising fibers derived from a phenolic resin and have, on average, surface areas of ∼1500–2500 m^2 g^{-1} [142, 143]. Much of the research has focused on material modifications to enhance electrosorption capacity [117, 144–148], which depends on the surface area and pore structure, electrical connectivity, and surface chemistry. For instance, the electrosorption capability was increased three-fold compared to unmodified ACCs through the incorporation of titania that decreased the physical adsorption of salt on the electrode [144].

Surface modifications such as acid etches have also proved to greatly enhance ion capture in ACCs. Oh *et al* demonstrated that the efficiency of activated carbon cloths could be improved through surface modification with KOH and HNO_3 solutions which increases the presence of carboxyl, carbonyl, and hydroxyl functional groups on the carbon surface, aiding in the adsorption [117]. For a 2000 $\mu S\,cm^{-1}$ NaCl solution (approximately 20 mM) and with voltages ranging from 1.0 to 1.5 V, the fraction of salt removed increased from 41% to 53% for the standard ACC, 44% to 58% for the KOH treated ACC, and 51% to 67% for the HNO_3 treatment. They further concluded that the surface carbonyl groups added by the HNO_3 modification increased the efficiency through enhanced double layer electrosorption and also by Faradaic reactions.

4.2.4. Carbon nanotubes and nanofibers (CNT/CNF). Various studies on effective ion capture have also been carried out using CNT/CNF composite electrodes fabricated by CVD [116, 149–151]. The CNT/CNF electrodes have a morphological advantage over standard activated carbon and ACCs with a larger number of mesopores and macropores, thereby increasing electrosorption performance [149]. Unlike micropores (typically smaller than 2 nm) where overlapping EDLs effectively reduce the accessible pore diameter and hinder transport of ions into the pores, the larger mesopores and macropores are not significantly affected by overlapping EDLs. Although the specific surface area of the CNT/CNF electrodes was reported to be smaller than the activated carbon

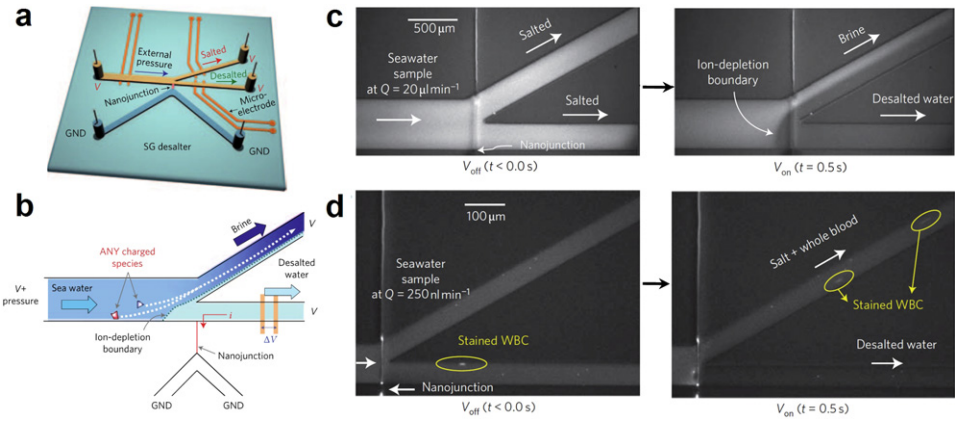

Figure 13. Schematic of the micro/nanofluidic desalination system (a) showing ion concentration polarization (b). (c) Fluorescence micrograph visualizing the desalination processes where the introduced seawater was divided into brine and desalinated streams. (d) Fluorescent dyes (representing salts) and white blood cells (representing micron-sized particles) passed only through the brine stream when voltage was applied. Adapted with permission from [154] (Copyright 2010, Nature Publishing Group).

(210 m^2 g^{-1} compared to 1500 m^2 g^{-1}), the electrosorptive capacity was 56.8 μmol g^{-1} as compared to 83 μmol g^{-1} for ACC [116].

4.2.5. Ordered mesoporous carbons. The microstructure of the electrode material, as suggested by the CNT/CNF studies, may prove to have a significant effect on electrosorption. Ordered mesoporous carbon materials can achieve regular, ordered pores ranging between 3–25 nm. These materials are synthesized by impregnating either a mesoporous silica or similar type structure with carbon. After the base material is removed, a highly ordered mesoporous carbon material remains [152, 153]. While mesoporous materials may be expected to have a high electrosorptive capacity, Li *et al* demonstrated with ordered mesoporous carbons (surface area 1000–1500 m^2 g^{-1}) that even for a smaller capacitance, the material exhibited increased ion capture [153]. Although the mechanism is unclear, this phenomenon was attributed to a more ordered structure aiding the transport of ions. This anomaly has critical implications for future material design and testing. Not only may materials with a more ordered pore structure facilitate the transport of ions into the pores, but it also signifies that standard electrochemical testing techniques to obtain capacitance measurements may not adequately describe material performance in a CDI system.

4.3. Summary

Understanding ion transport within nanometers of the electrode–electrolyte interface can greatly enhance the ability to design materials and structures to increase ion capture for CDI. Opportunities exist in tailoring material geometry and performing systematic studies to isolate transport limitations. Investigating the effect of pore size on the electrosorption and transport of ions will offer insights into electrode capacity and charging times. On the macroscopic level, optimizing the pore geometry and electrode structure could enhance the efficiency of CDI.

In addition to opportunities in CDI, the ability to fabricate structures at the micro- and nano-length scales has also resulted in other new electric-field-based separation methods for water desalination. Kim *et al* recently developed a method for membraneless desalination using ionic concentration polarization originally used for preconcentration of biological samples [154]. The desalination device consists of two microchannels connected by nanochannels (figure 13). Application of a voltage bias across the nanochannels resulted in depletion of ions and molecules at the microchannel/nanochannel interface. By dividing the flow in the microchannel into two, a stream of desalinated water and a stream of brine were obtained. This architecture does not expose the nanochannels (selective material) to the feedwater, which may have implications on the fouling resistance of the device. This device desalinated pretreated seawater from a concentration of ∼500 mM to a concentration of ∼3 mM. This method was reported to have an energy requirement of only 3.75 kWh m^{-3}, which is comparable to the energy requirement of existing RO systems. While this non-linear phenomenon under the application of a large voltage bias promises efficient desalination, the mechanism of transport is complex and further development is required for commercial applications.

5. Phase-change-based processes

Phase-change-based water desalination technologies, in particular MSF and MED, currently account for over 40% of the world's desalination capacity [155]. The benefits of these thermal desalination processes include robust operation, high purity permeate, energy usage nearly independent of feedwater salt concentrations, and large capacity. However, these desalination plants require more energy than RO plants due to the high heat of vaporization for water. Therefore, new thermal desalination plants are typically installed where the cost of energy is low, waste energy is readily available, or feedwater salinity is high [3].

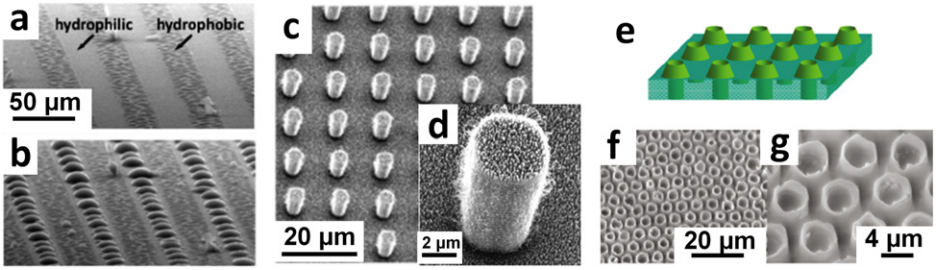

Figure 14. Condensation behavior on alternatively patterned hydrophobic and hydrophilic surfaces showing the dry surface (a) and following condensation (b). Adapted with permission from [171] (Copyright 2009, American Institute of Physics). (c) Two-tiered structures of superhydrophobic surface for dropwise condensation. (d) Magnified image of a single micropillar in (c). Adapted with permission from [170] (Copyright 2007, American Institute of Physics). Glass made nanospiked microtubes with a hydrophobic surface modification for membrane distillation (e), showing SEM images (f) and (g). Adapted with permission from [175] (Copyright 2009, American Chemical Society).

MSF utilizes several stages of evaporation by flashing water into sequential chambers under decreasing pressures; the resulting vapor is condensed by cooler feed water pumped through condenser tubes and collected as desalinated water (figure 1). MED plants comprise several (4–12) evaporators; vapor from one evaporator is directed to the following evaporator and serves as the heat input to evaporate the brine (figure 1) [156]. The advantages of MSF include simple design and available expertise in the operation and construction of these systems; scale formation, biofouling, and corrosion problems have been largely addressed for MSF systems [157–160]. It is very likely that MSF will remain widely used for many years to come because of these advantages. The pumping energy requirement in MED is lower than that in MSF since water passes through an evaporator only once in MED [5]. However, MED is more prone to scale formation, which limits the operating temperature and performance of these plants. This limitation can be partly overcome by scale control treatment methods such as acid treatment and additives [161]. Recent advances in MED include new heat exchanger designs with higher overall heat transfer coefficients and reduced heat transfer surface areas as compared to MSF. These improvements have enabled MED to become competitive with MSF for desalination. Thus, in addition to approaches to mitigate scaling, new heat exchanger designs that minimize capital cost for a given capacity, decrease pumping power, and improve overall heat transfer coefficients can improve the performance of MED and MSF systems.

Apart from MSF and MED, other techniques such as vapor compression [162], humidification–dehumidification (HDH) [163], membrane distillation [164], and solar distillation [165] are also promising for smaller scale applications [166–168]. Vapor compression utilizes mechanically or thermally compressed vapor to supply energy for seawater evaporation; the condensed vapor through heat exchange with seawater is collected as desalinated water. HDH reproduces the rain cycle, first humidifying air with heated seawater. The humid air is then introduced to a dehumidifier where desalinated water is obtained by condensation through heat exchange with supplied cold feedwater. Membrane distillation is also a thermally driven desalination process, where elevated (50–90 °C) temperature feedwater and low temperature desalinated water are introduced on either sides of a hydrophobic porous membrane. Feedwater evaporates and condenses into the cooler water on the other side of the membrane. While low-grade energy sources including solar energy can be utilized in membrane distillation, low efficiency, low flux, and membrane wetting currently limit the use of this process [169].

In phase-change-based desalination processes, advances in materials and designs for improved heat transfer and control over evaporation and condensation can potentially enhance the performance of these systems. Recent developments indicate that nanostructured materials can enhance heat transfer by control of vaporization and condensation processes.

5.1. Nanostructured materials for phase-change-based processes

Recent developments in nanostructure engineering have offered new opportunities to enhance heat transfer through phase-change processes [170–173]. For example, multi-scale nanostructured materials with controlled surface chemistry can potentially enhance condensation heat transfer via dropwise condensation compared to conventional film condensation using superhydrophobic surfaces. Varanasi *et al* [171] isolated water nucleation to the top of microstructures using surface modifications to promote condensate drop removal (figures 14(a) and (b)). Chen *et al* [170] developed two-tiered structures with nanotubes on micromachined posts to mimic the multi-scale structure of the lotus leaf, which allows the surfaces to be self-cleaning and superhydrophobic (figures 14(c) and (d)) [174]. While these studies are still in the preliminary research stages, where heat transfer measurements need to be obtained, they promise new opportunities to enhance phase-change-based desalination systems if processes for the large-scale manufacture of such surfaces are developed.

In addition to enhanced condensation heat transfer, nanostructured materials can be useful for controlling the wetting and transport of vapor. Ma *et al* [175] created glass membranes with nanospiked superhydrophobic microchannels for membrane distillation (figures 14(e)–(g)). This membrane provided large, non-tortuous pores enabling higher mass flux compared to polymeric membranes. The nanospiked structure also moderated fouling issues by reducing the contact

area of the water and membrane. More recently, Lee and Karnik proposed a membrane comprising short, hydrophobic nanopores that enable evaporation and condensation driven by a pressure difference similar to RO [176]. Theoretical modeling indicated the possibility of improved flux compared to polymeric RO membranes for moderately elevated temperatures.

5.2. Summary

In contrast to RO and ED which directly employ micro- to nanoscale transport phenomena for desalination, MSF and MED operate mostly in the macroscopic regime. These technologies would benefit from improved evaporation and condensation heat transfer. New nanostructured surfaces offer the potential for enhanced heat transfer rates for condensation as well as evaporation, which may result in the improved efficiency of these desalination plants. Improved understanding of heat transfer on nanostructured surfaces as well as scalable manufacturing techniques are required before such surfaces can be implemented. Meanwhile, phase-change-based techniques such as membrane distillation that rely on transport at small length scales could be advanced more readily by implementing new nanostructured materials.

6. Conclusions

There is a growing need for improving desalination technologies as the demand for clean water grows, energy costs rise, and natural resources diminish. As current desalination technologies reach maturation, nanostructured materials will play an increasingly important role in realizing next-generation desalination technologies. Unprecedented control of surface structure and chemistry resulting from progress in nanofabrication techniques provides new opportunities to understand nanoscale transport phenomena and to harness nanostructured materials to realize macroscopic effects. In this review, we have focused on these aspects and their potential to impact desalination technologies in the future.

RO membrane performance has improved significantly over the past decade due to system-level improvements such as energy recovery and feedwater pre-treatment, as well as advances in membrane materials. However, current polymeric RO membranes have low flux rates, and also suffer from fouling and poor chemical resistance. New nanostructured materials, such as CNTs, zeolites, and graphene, may serve as ideal membranes consisting of rigid, size-selective pores that operate as molecular sieves, permitting high permeabilities compared to existing membranes. Much work is still required before these membranes become commercially viable, including a fundamental understanding of transport processes, cost reduction, pore size optimization, and system-level integration, but the promise of reduced capital and operating costs should encourage the development of these new materials.

While ED has matured as a niche desalination technology, CDI is an emerging desalination technology for brackish water utilizing the electromigration and electrosorption of salt ions. Since the efficiency of CDI weighs heavily on the design of the electrodes and electrode structure, most research has focused on developing electrodes with a high surface area, good conductivity, and controlled Faradaic reactions. Nanostructured materials, such as carbon aerogels, activated carbon, ACC, CNT/CNF, and ordered mesoporous carbons, are being investigated as CDI electrode materials. However, the design of the electrodes requires an understanding of ionic transport phenomena and electrochemistry spanning multiple length scales. This area needs further research, which is a prerequisite for optimizing electrode configurations. Advances in microfluidics and the ability to study ionic transport under controlled conditions may lead to an increased understanding of CDI and novel charge-based desalination techniques.

Phase-change desalination processes were the first to be established commercially of all of the desalination techniques and now account for over 40% of the world's desalination capacity. However, the major drawback of phase-change processes is the high heat of vaporization required to initiate phase separation of the salt and water molecules. Improving the performance of heat exchangers using nanostructured materials holds promise for potentially decreasing the capital cost and improving the efficiency of these processes. Similarly, control of wetting, evaporation, condensation, and vapor-phase transport promises improvements in membrane distillation and new phase-change-based desalination techniques.

While there is still a need for fundamental research, the impact of nanostructured materials is already evident by a number of start-up companies that utilize such materials for desalination [177]. The rapid advances in understanding nanoscale transport phenomena and the development of nanostructured materials combined with significant interest in commercialization, will certainly help ensure that the demand for clean water is met in an efficient, affordable, and sustainable manner for future generations.

Acknowledgments

The authors would like to thank the King Fahd University of Petroleum and Minerals in Dhahran, Saudi Arabia, for funding the research reported in this paper through the Center for Clean Water and Clean Energy at MIT and KFUPM.

References

[1] Shannon M A *et al* 2008 Science and technology for water purification in the coming decades *Nature* **452** 301–10
[2] El-Dessouky H and Ettouney H 2002 Teaching desalination—a multidiscipline engineering science *Heat Transfer Eng.* **23** 1–3
[3] Miller J E 2003 Review of water resources and desalination technologies *Sandia National Laboratories Report, SAND2003-0800*
[4] National Research Council (US) Committee on Advancing Desalination Technology and National Academies Press (US) 2008 *Desalination: A National Perspective* vol xiv (Washington, DC: National Academies Press) p 298
[5] State of Desalination 2009 *IDA World Congress on Desalination and Water Reuse* Dubai

[6] Greenlee L F *et al* 2009 Reverse osmosis desalination: water sources, technology, and today's challenges *Water Res.* **43** 2317–48

[7] Potts D E, Ahlert R C and Wang S S 1981 A critical-review of fouling of reverse-osmosis membranes *Desalination* **36** 235–64

[8] Eijkel J C T and van den Berg A 2005 Nanofluidics: what is it and what can we expect from it? *Microfluid. Nanofluid.* **1** 249–67

[9] Gogotsi Y 2006 *Carbon nanomaterials* (Boca Raton, FL: Taylor and Francis) p 326

[10] Baughman R H, Zakhidov A A and de Heer W A 2002 Carbon nanotubes—the route toward applications *Science* **297** 787–92

[11] Novoselov K S *et al* 2004 Electric field effect in atomically thin carbon films *Science* **306** 666–9

[12] Sahoo S K and Labhasetwar V 2003 Nanotech approaches to delivery and imaging drug *Drug Discov. Today* **8** 1112–20

[13] Lu A H, Salabas E L and Schuth F 2007 Magnetic nanoparticles: synthesis, protection, functionalization, and application *Angew. Chem. Int. Edn* **46** 1222–44

[14] Arico A S *et al* 2005 Nanostructured materials for advanced energy conversion and storage devices *Nat. Mater.* **4** 366–77

[15] Murphy C J *et al* 2005 Anisotropic metal nanoparticles: synthesis, assembly, and optical applications *J. Phys. Chem.* B **109** 13857–70

[16] O'Farrell N, Houlton A and Horrocks B R 2006 Silicon nanoparticles: applications in cell biology and medicine *Int. J. Nanomed.* **1** 451–72

[17] Fritzmann C *et al* 2007 State-of-the-art of reverse osmosis desalination *Desalination* **216** 1–76

[18] Li D and Wang H T 2010 Recent developments in reverse osmosis desalination membranes *J. Mater. Chem.* **20** 4551–66

[19] Lee K P, Arnot T C and Mattia D 2011 A review of reverse osmosis membrane materials for desalination—development to date and future potential *J. Membr. Sci.* **370** 1–22

[20] Malaeb L and Ayoub G M 2011 Reverse osmosis technology for water treatment: state of the art review *Desalination* **267** 1–8

[21] El-Dessouky H T, Ettouney H M and Al-Roumi Y 1999 Multi-stage flash desalination: present and future outlook *Chem. Eng. J.* **73** 173–90

[22] Al-Shammiri M and Safar M 1999 Multi-effect distillation plants: state of the art *Desalination* **126** 45–59

[23] Goosen M F A *et al* 2004 Fouling of reverse osmosis and ultrafiltration membranes: a critical review *Sep. Sci. Technol.* **39** 2261–97

[24] Baker J S and Dudley L Y 1998 Biofouling in membrane systems—a review *Desalination* **118** 81–9

[25] Savage N and Diallo M S 2005 Nanomaterials and water purification: opportunities and challenges *J. Nanopart. Res.* **7** 331–42

[26] Theron J, Walker J A and Cloete T E 2008 Nanotechnology and water treatment: applications and emerging opportunities *Crit. Rev. Microbiol.* **34** 43–69

[27] Khawaji A D, Kutubkhanah I K and Wie J M 2008 Advances in seawater desalination technologies *Desalination* **221** 47–69

[28] Hahn W J 1986 Measurements and control in freeze desalination plants *Desalination* **59** 321–41

[29] Sonune A and Ghate R 2004 Developments in wastewater treatment methods *Desalination* **167** 55–63

[30] Kabay N *et al* 2008 Adsorption-membrane filtration (AMF) hybrid process for boron removal from seawater: an overview *Desalination* **223** 38–48

[31] Kabay N *et al* 2007 Removal of boron from seawater by selective ion exchange resins *React. Funct. Polym.* **67** 1643–50

[32] Probstein R F 2003 *Physicochemical Hydrodynamics: An Introduction* 2nd edn vol xv (Hoboken, NJ: Wiley-Interscience) p 400

[33] Soltanieh M and Gill W N 1981 Review of reverse-osmosis membranes and transport models *Chem. Eng. Commun.* **12** 279–363

[34] Wijmans J G and Baker R W 1995 The solution–diffusion model—a review *J. Membr. Sci.* **107** 1–21

[35] Paul D R 2004 Reformulation of the solution–diffusion theory of reverse osmosis *J. Membr. Sci.* **241** 371–86

[36] Spiegler K S and El-Sayed Y M 2001 The energetics of desalination processes *Desalination* **134** 109–28

[37] Sablani S S *et al* 2001 Concentration polarization in ultrafiltration and reverse osmosis: a critical review *Desalination* **141** 269–89

[38] Kimura S and Souriraj S 1967 Analysis of data in reverse osmosis with porous cellulose acetate membranes used *AIChE J.* **13** 497–512

[39] DOW Water Solutions FILMTEC Membranes, I 2011 *Product Information Catalog* www.rosystems.com/pdf/Filmtec-Membranes/filmtecliterature.pdf (accessed on June 7, 2011)

[40] Koch Membrane Systems Technical Literature: Reverse Osmosis http://www.kochmembrane.com/support_ro_lit.html (accessed on June 7, 2011)

[41] GE Water and Process Technologies Desalination Membrane Literature http://www.gewater.com/what_we_do/water_scarcity/desalination.jsp (accessed on June 7, 2011)

[42] TriSep Corporation Desalination Literature http://www.trisep.com (accessed on June 7, 2011)

[43] Jeong B *et al* 2007 Interfacial polymerization of thin film nanocomposites: a new concept for reverse osmosis membranes *J. Membr. Sci.* **294** 1–7

[44] Li L X and Lee R 2009 Purification of produced water by ceramic membranes: material screening, process design and economics *Sep. Sci. Technol.* **44** 3455–84

[45] Fornasiero F *et al* 2008 Ion exclusion by sub-2 nm carbon nanotube pores *Proc. Natl Acad. Sci. USA* **105** 17250–5

[46] Holt J K *et al* 2006 Fast mass transport through sub-2 nm carbon nanotubes *Science* **312** 1034–7

[47] Vandezande P, Gevers L E M and Vankelecom I F J 2008 Solvent resistant nanofiltration: separating on a molecular level *Chem. Soc. Rev.* **37** 365–405

[48] Han J Y, J P Fu and Schoch R B 2008 Molecular sieving using nanofilters: past, present and future *Lab on a Chip* **8** 23–33

[49] Grunwald E 1997 *Thermodynamics of Molecular Species* (New York: Wiley) p 319

[50] Song C and Corry B 2009 Intrinsic ion selectivity of narrow hydrophobic pores *J. Phys. Chem.* B **113** 7642–9

[51] Li L *et al* 2004 Desalination by reverse osmosis using MFI zeolite membranes *J. Membr. Sci.* **243** 401–4

[52] Li L *et al* 2008 Counter ions on the reverse osmosis through MFI zeolite membranes: implications for produced water desalination *Desalination* **228** 217–25

[53] Jiang D E, Cooper V R and Dai S 2009 Porous graphene as the ultimate membrane for gas separation *Nano Lett.* **9** 4019–24

[54] Bai J *et al* 2010 Graphene nanomesh *Nat. Nanotechnol.* **5** 190–4

[55] Sint K, Wang B and Kral P 2008 Selective ion passage through functionalized graphene nanopores *J. Am. Chem. Soc.* **130** 16448–9

[56] Čejka J 2007 *Introduction to Zeolite Science and Practice* 3rd edn (New York: Elsevier) p 1058

[57] Bailey S *et al* 1999 A review of potentially low-cost sorbents for heavy metals *Water Res.* **33** 2469–79

[58] Lai Z, Tsapatsis M and Nicolich J P 2004 Siliceous ZSM-5 membranes by secondary growth of b-oriented seed layers *Adv. Funct. Mater.* **14** 716–29

[59] Murad S M and Lin J C 2002 Using thin zeolite membranes and external electric fields to separate supercritical aqueous electrolyte solutions *Ind. Eng. Chem. Res.* **41** 1076–83

[60] Murad S, Oder K and Lin J 1998 Molecular simulation of osmosis, reverse osmosis, and electro-osmosis in aqueous and methanolic electrolyte solutions *Mol. Phys.* **95** 401–8

[61] Li L *et al* 2008 Influence of counter ions on the reverse osmosis through MFI zeolite membranes: implications for produced water desalination *Desalination* **228** 217–25

[62] Iijima S 1991 Helical microtubules of graphitic carbon *Nature* **354** 56–8

[63] Dresselhaus M S, Dresselhaus G and Saito R 1995 Physics of carbon nanotubes *Carbon* **33** 883–91

[64] Frank S *et al* 1998 Carbon nanotube quantum resistors *Science* **280** 1744–6

[65] Niyogi S *et al* 2002 Chemistry of single-walled carbon nanotubes *Acc. Chem. Res.* **35** 1105–13

[66] Nygard J, Cobden D H and Lindelof P E 2000 Kondo physics in carbon nanotubes *Nature* **408** 342–6

[67] Tans S J *et al* 1997 Individual single-wall carbon nanotubes as quantum wires *Nature* **386** 474–7

[68] Wang J 2005 Carbon-nanotube based electrochemical biosensors: a review *Electroanalysis* **17** 7–14

[69] Ugarte D, Chatelain A and deHeer W A 1996 Nanocapillarity and chemistry in carbon nanotubes *Science* **274** 1897–9

[70] Wang J, Musameh M and Lin Y H 2003 Solubilization of carbon nanotubes by Nafion toward the preparation of amperometric biosensors *J. Am. Chem. Soc.* **125** 2408–9

[71] Zheng M *et al* 2003 DNA-assisted dispersion and separation of carbon nanotubes *Nat. Mater.* **2** 338–42

[72] Bahr J L and Tour J M 2002 Covalent chemistry of single-wall carbon nanotubes *J. Mater. Chem.* **12** 1952–8

[73] Arjmandi N, Sasanpour P and Rashidian B 2009 CVD synthesis of small-diameter single-walled carbon nanotubes on silicon *Sci. Iran. Trans.* D **16** 61–4

[74] Lukic B *et al* 2005 Catalytically grown carbon nanotubes of small diameter have a high Young's modulus *Nano Lett.* **5** 2074–7

[75] Pint C L *et al* 2008 Synthesis of high aspect-ratio carbon nanotube 'flying carpets' from nanostructured flake substrates *Nano Lett.* **8** 1879–83

[76] Sun L F *et al* 2000 Materials—creating the narrowest carbon nanotubes *Nature* **403** 384

[77] Cheung C L *et al* 2002 Diameter-controlled synthesis of carbon nanotubes *J. Phys. Chem.* B **106** 2429–33

[78] Majumder M *et al* 2005 Nanoscale hydrodynamics—enhanced flow in carbon nanotubes *Nature* **438** 44

[79] Joseph S and Aluru N R 2008 Why are carbon nanotubes fast transporters of water? *Nano Lett.* **8** 452–8

[80] Falk K *et al* 2010 Molecular origin of fast water transport in carbon nanotube membranes: superlubricity versus curvature dependent friction *Nano Lett.* **10** 4067–73

[81] Hummer G, Rasaiah J C and Noworyta J P 2001 Water conduction through the hydrophobic channel of a carbon nanotube *Nature* **414** 188–90

[82] Kolesnikov A I *et al* 2004 Anomalously soft dynamics of water in a nanotube: a revelation of nanoscale confinement *Phys. Rev. Lett.* **93** 035503

[83] Hinds B J *et al* 2004 Aligned multiwalled carbon nanotube membranes *Science* **303** 62–5

[84] Yu M *et al* 2009 High density, vertically-aligned carbon nanotube membranes *Nano Lett.* **9** 225–9

[85] Geim A K 2009 Graphene: status and prospects *Science* **324** 1530–4

[86] Allen M J, Tung V C and Kaner R B 2010 Honeycomb carbon: a review of graphene *Chem. Rev.* **110** 132–45

[87] Lee C *et al* 2008 Measurement of the elastic properties and intrinsic strength of monolayer graphene *Science* **321** 385–8

[88] Bunch J S *et al* 2008 Impermeable atomic membranes from graphene sheets *Nano Lett.* **8** 2458–62

[89] Bae S *et al* 2010 Roll-to-roll production of 30 inch graphene films for transparent electrodes *Nat. Nanotechnol.* **5** 574–8

[90] Meyer J C *et al* 2008 Direct imaging of lattice atoms and topological defects in graphene membranes *Nano Lett.* **8** 3582–6

[91] Saito M, Yamashita K and Oda T 2007 Magic numbers of graphene multivacancies *Japan. J. Appl. Phys.* **46** L1185–7

[92] Suk M E and Aluru N R 2010 Water transport through ultrathin graphene *J. Phys. Chem. Lett.* **1** 1590–4

[93] Chen J-H *et al* 2009 Defect scattering in graphene *Phys. Rev. Lett.* **102** 236805

[94] Zhang J *et al* 2003 Effect of chemical oxidation on the structure of single-walled carbon nanotubes *J. Phys. Chem.* B **107** 3712–8

[95] Fischbein M D and Drndic M 2008 Electron beam nanosculpting of suspended graphene sheets *Appl. Phys. Lett.* **93** 113107

[96] Hashimoto A *et al* 2004 Direct evidence for atomic defects in graphene layers *Nature* **430** 870–3

[97] Inui N *et al* 2010 Molecular dynamics simulations of nanopore processing in a graphene sheet by using gas cluster ion beam *Appl. Phys.* A **98** 787–94

[98] Krasheninnikov A V *et al* 2001 Formation of ion-irradiation-induced atomic-scale defects on walls of carbon nanotubes *Phys. Rev.* B **6324** 245405

[99] Lucchese M M *et al* 2010 Quantifying ion-induced defects and Raman relaxation length in graphene *Carbon* **48** 1592–7

[100] Krasheninnikov A V, Nordlund K and Keinonen J 2002 Production of defects in supported carbon nanotubes under ion irradiation. *Phys. Rev.* B **65** 165423

[101] Pomoell J A V *et al* 2004 Ion ranges and irradiation-induced defects in multiwalled carbon nanotubes *J. Appl. Phys.* **96** 2864–71

[102] Wei D C *et al* 2009 Synthesis of N-doped graphene by chemical vapor deposition and its electrical properties *Nano Lett.* **9** 1752–58

[103] Garaj S *et al* 2010 Graphene as a subnanometre trans-electrode membrane *Nature* **467** 190–3

[104] Merchant C A *et al* 2010 DNA Translocation through graphene nanopores *Nano Lett.* **10** 2915–21

[105] Schneider G F *et al* 2010 DNA Translocation through Graphene Nanopores *Nano Lett.* **10** 3163–7

[106] Zhou M J *et al* 2007 New type of membrane material for water desalination based on a cross-linked bicontinuous cubic lyotropic liquid crystal assembly *J. Am. Chem. Soc.* **129** 9574–82

[107] Striemer C C *et al* 2007 Charge- and size-based separation of macromolecules using ultrathin silicon membranes *Nature* **445** 749–53

[108] Gong X J *et al* 2007 A charge-driven molecular water pump *Nat. Nanotechnol.* **2** 709–12

[109] Murata K *et al* 2000 Structural determinants of water permeation through aquaporin-1 *Nature* **407** 599–605

[110] Zuo G C *et al* 2010 Transport properties of single-file water molecules inside a carbon nanotube biomimicking water channel *ACS Nano* **4** 205–10

[111] Ho D *et al* 2004 Hybrid protein-polymer biomimetic membranes *IEEE Trans. Nanotechnol.* **3** 256–63

[112] Oren Y 2008 Capacitive delonization (CDI) for desalination and water treatment—past, present and future (a review) *Desalination* **228** 10–29

[113] Christen K 2006 Desalination technology could clean up wastewater from coal-bed methane production *Environ. Sci. Technol.* **40** 639

[114] Anderson M A, Cudero A L and Palma J 2010 Capacitive deionization as an electrochemical means of saving energy and delivering clean water. Comparison to present desalination practices: will it compete? *Electrochim. Acta* **55** 3845–56

[115] Xu T W 2005 Ion exchange membranes: state of their development and perspective *J. Membr. Sci.* **263** 1–29

[116] Wang X Z *et al* 2006 Electrosorption of ions from aqueous solutions with carbon nanotubes and nanofibers composite film electrodes *Appl. Phys. Lett.* **89** 053127

[117] Oh H J *et al* 2006 Nanoporous activated carbon cloth for capacitive deionization of aqueous solution *Thin Solid Films* **515** 220–5

[118] Li J *et al* 2006 Studies on preparation and performances of carbon aerogel electrodes for the application of supercapacitor *J. Power Sources* **158** 784–8

[119] Hampsey J E *et al* 2005 Templating synthesis of ordered mesoporous carbon particles *Carbon* **43** 2977–82

[120] Bazant M, Thornton K and Ajdari A 2004 Diffuse-charge dynamics in electrochemical systems *Phys. Rev.* E **70** 021506

[121] Bazant M Z *et al* 2009 Nonlinear electrokinetics at large voltages *New J. Phys.* **11** 075016

[122] Kilic M S, Bazant M Z and Ajdari A 2007 Steric effects in the dynamics of electrolytes at large applied voltages. I. Double-layer charging *Phys. Rev.* E **75** 021502

[123] Kilic M S, Bazant M Z and Ajdari A 2007 Steric effects in the dynamics of electrolytes at large applied voltages. II. Modified Poisson–Nernst–Planck equations *Phys. Rev.* E **75** 021503

[124] Biesheuvel P M and Bazant M Z 2010 Nonlinear dynamics of capacitive charging and desalination by porous electrodes. *Phys. Rev.* E **81** 031502

[125] Biesheuvel P M, van Limpt B and van der Wal A 2009 Dynamic adsorption/desorption process model for capacitive deionization *J. Phys. Chem.* C **113** 5636–40

[126] Johnson A M and Newman J 1971 Desalting by means of porous carbon electrodes *J. Electrochem. Soc.* **118** 510

[127] Farmer J *et al* 1996 Capacitive deionization of NH_4ClO_4 solutions with carbon aerogel electrodes *J. Appl. Electrochem.* **26** 1007–18

[128] Farmer J *et al* 1996 Capacitive deionization of NaCl and $NaNO_3$ solutions with carbon aerogel electrodes *J. Electrochem. Soc.* **143** 159–69

[129] Pekala R W *et al* 1998 Carbon aerogels for electrochemical applications *J. Non-Cryst. Solids* **225** 74–80

[130] Farmer J C *et al* 1995 The use of capacitive deionization with carbon aerogel electrodes to remove inorganic contaminants from water *Electric Power Research Institute low-level waste conference (Orlando, FL, Jul 1995)*

[131] Gabelich C, Tran T and Suffet I 2002 Electrosorption of inorganic salts from aqueous solution using carbon aerogels *Environ. Sci. Technol.* **36** 3010–9

[132] Hwang S and Hyun S 2004 Capacitance control of carbon aerogel electrodes *J. Non-Cryst. Solids* **347** 238–45

[133] Jung H-H *et al* 2007 Capacitive deionization characteristics of nanostructured carbon aerogel electrodes synthesized via ambient drying *Desalination* **216** 377–85

[134] Xu P *et al* 2008 Treatment of brackish produced water using carbon aerogel-based capacitive deionization technology *Water Res.* **42** 2605–17

[135] Yang C *et al* 2005 Capacitive deionization of NaCl solution with carbon aerogel–silica gel composite electrodes *Desalination* **174** 125–33

[136] Yang K *et al* 2001 Electrosorption of ions from aqueous solutions by carbon aerogel: an electrical double-layer model *Langmuir* **17** 1961–9

[137] Gamby J *et al* 2001 Studies and characterisations of various activated carbons used for carbon/carbon supercapacitors *J. Power Sources* **101** 109–16

[138] Avraham E *et al* 2009 Limitations of charge efficiency in capacitive deionization II. On the behavior of cdi cells comprising two activated carbon electrodes *J. Electrochem. Soc.* **156** P157–62

[139] Zou L, Morris G and Qi D 2008 Using activated carbon electrode in electrosorptive deionisation of brackish water *Desalination* **225** 329–40

[140] Park K-K *et al* 2007 Development of a carbon sheet electrode for electrosorption desalination *Desalination* **206** 86–91

[141] Lee J-B *et al* 2009 Desalination performance of a carbon-based composite electrode *Desalination* **237** 155–61

[142] Lee J B *et al* 2006 Desalination of a thermal power plant wastewater by membrane capacitive deionization. *Desalination* **196** 125–34

[143] Ayranci E and Duman O 2005 Adsorption behaviors of some phenolic compounds onto high specific area activated carbon cloth *J. Hazard. Mater.* **124** 125–32

[144] Ryoo M, Kim J and Seo G 2003 Role of titania incorporated on activated carbon cloth for capacitive deionization of NaCl solution *J. Colloid Interface Sci.* **264** 414–9

[145] Ryoo M and Seo G 2003 Improvement in capacitive deionization function of activated carbon cloth by titania modification *Water Res.* **37** 1527–34

[146] Ahn H-J *et al* 2007 Nanostructured carbon cloth electrode for desalination from aqueous solutions *Mater. Sci. Eng.* A **449** 841–5

[147] Avraham E *et al* 2009 Limitation of charge efficiency in capacitive deionization *J. Electrochem. Soc.* **156** P95–9

[148] Noked M *et al* 2009 The rate-determining step of electroadsorption processes into nanoporous carbon electrodes related to water desalination *J. Phys. Chem.* C **113** 21319–27

[149] Wang X Z *et al* 2006 Electrosorption of NaCl solutions with carbon nanotubes and nanofibers composite film electrodes *Electrochem. Solid State* **9** E23–6

[150] Pan L *et al* 2009 Electrosorption of anions with carbon nanotube and nanofibre composite film electrodes *Desalination* **244** 139–43

[151] Li H *et al* 2008 Electrosorptive desalination by carbon nanotubes and nanofibres electrodes and ion-exchange membranes *Water Res.* **42** 4923–8

[152] Ryoo R *et al* 2001 Ordered mesoporous carbons *Adv. Mater.* **13** 677–81

[153] Li L X *et al* 2009 Ordered mesoporous carbons synthesized by a modified sol–gel process for electrosorptive removal of sodium chloride *Carbon* **47** 775–81

[154] Kim S J *et al* 2010 Direct seawater desalination by ion concentration polarization *Nat. Nanotechnol.* **5** 297–301

[155] El-Dessouky H *et al* 2002 Evaluation of steam jet ejectors *Chem. Eng. Process.* **41** 551–61

[156] Raluy G, Serra L and Uche J 2006 Life cycle assessment of MSF, MED and RO desalination technologies *Energy* **31** 2361–72

[157] Butt F *et al* 1985 Field trials of hybrid acid-additive treatment for control of scale in msf plants *Desalination* **54** 307–20

[158] Eldin A M S and Mohammed R A 1994 Brine and scale chemistry in MSF distillers *Desalination* **99** 73–111

[159] Hamed O A *et al* 1999 The performance of different anti-sealants in multi-stage flash distillers *Desalination* **123** 185–94
[160] Neofofistou E and Demadis K D 2004 Use of antiscalants for mitigation of silica (SiO_2) fouling and deposition: fundamentals and applications in desalination systems *Desalination* **167** 257–72
[161] Patel S and Finan M A 1999 New antifoulants for deposit control in MSF and MED plants *Desalination* **124** 63–74
[162] Ettouney H, El-Dessouky H and Al-Roumi Y 1999 Analysis of mechanical vapour compression desalination process *Int. J. Energy Res.* **23** 431–51
[163] Narayan G P *et al* 2010 The potential of solar-driven humidification–dehumidification desalination for small-scale decentralized water production *Renew. Sustain. Energy Rev.* **14** 1187–201
[164] Lawson K W and Lloyd D R 1997 Membrane distillation *J. Membr. Sci.* **124** 1–25
[165] Fath H E S 1998 Solar distillation: a promising alternative for water provision with free energy, simple technology and a clean environment *Desalination* **116** 45–56
[166] Al-Obaidani S *et al* 2008 Potential of membrane distillation in seawater desalination: thermal efficiency, sensitivity study and cost estimation *J. Membr. Sci.* **323** 85–98
[167] Kalogirou S A 2005 Seawater desalination using renewable energy sources *Prog. Energy Combus. Sci.* **31** 242–81
[168] Semiat R 2008 Energy issues in desalination processes *Environ. Sci. Technol.* **42** 8193–201
[169] El-Bourawi M S *et al* 2006 A framework for better understanding membrane distillation separation process *J. Membr. Sci.* **285** 4–29
[170] Chen Z H *et al* 2007 Dropwise condensation on superhydrophobic surfaces with two-tier roughness *Appl. Phys. Lett.* **90** 173108
[171] Varanasi K K *et al* 2009 Spatial control in the heterogeneous nucleation of water *Appl. Phys. Lett.* **95** 094101
[172] Jones B J, McHale J P and Garimella S V 2009 The influence of surface roughness on nucleate pool boiling heat transfer *J. Heat Transf.-Trans. ASME* **131** 121009
[173] Wang H, Garimella S V and Murthy J Y 2007 Characteristics of an evaporating thin film in a microchannel *Int. J. Heat Mass Transf.* **50** 3933–42
[174] Patankar N A 2004 Mimicking the lotus effect: influence of double roughness structures and slender pillars *Langmuir* **20** 8209–13
[175] Ma Z Y *et al* 2009 Superhydrophobic membranes with ordered arrays of nanospiked microchannels for water desalination *Langmuir* **25** 5446–50
[176] Lee J and Karnik R 2010 Desalination of water by vapor-phase transport through hydrophobic nanopores *J. Appl. Phys.* **108** 044315
[177] Voith M 2009 Hard water *Chem. Eng. News* **87** 20–1